Journal of Theoretical and Applied Mechanics, Sofia, Vol.53 (2023) pp. 253-269
FLUID MECHANICS

EFFECT OF SLIP BOUNDARY CONDITIONS ON NONEQUILIBRIUM REACTING AIR FLOWS

L. SHAKUROVA[1,2*], I. ARMENISE[3], E. KUSTOVA[1,2]

[1]*Saint-Petersburg State University,*
7/9 Universitetskaya nab., St. Petersburg, 199034 Russia.

[2]*Federal Research Center "Computer Science and Control" of the Russian Academy of Sciences, 44-2 ul. Vavilova, Moscow, 119333, Russia*

[3]*CNR ISTP (Consiglio Nazionale delle Ricerche, Istituto per la Scienza e Tecnologia dei Plasmi), Sede Secondaria di Bari, Via Amendola 122/D, 70126, Bari, Italy*

[Received: 14 June 2023. Accepted: 4 July 2023]

doi: https://doi.org/10.55787/jtams.23.53.3.253

ABSTRACT: We study the effect of slip boundary conditions on the kinetics, dynamics, and heat transfer in a strongly nonequilibrium flow with coupled vibrational relaxation, state-specific gas-phase and surface reactions. Two types of kinetic boundary conditions are introduced: whereas one ensures number flux conservation, the second conserves the mass flux. Both kinetic boundary conditions are suitable for state-to-state flow simulations and take into account gain and loss of particles on the surface due to recombination and excitation/deactivation of vibrational states. On the basis of the proposed kinetic conditions, the velocity slip, temperature jump and species normal mass fluxes on the surface are derived. The models are used for numerical simulations of a five-component air mixture along stagnation line. The effects of kinetic boundary condition, diffusion model, accommodation coefficients are evaluated for different rarefaction degree. Important effect of diffusion model and temperature jump on the fluid-dynamic variables and heat flux is shown.

KEY WORDS: Heterogeneous reactions, accommodation coefficient, slip boundary conditions, state-to-state kinetics, nonequilibrium rarefied gas flow.

1 INTRODUCTION

This paper is dedicated to the 80-th anniversary of Professor Stefan Radev, who, in his early career during his stay in Saint Petersburg (ex. Leningrad) State University was working on rarefied gas dynamics (RGD). Since that time, great progress has

*Corresponding author e-mail: liya.shakurova.27@gmail.com

been made in the field of rarefied gases; advanced theoretical models and numerical tools were developed, and many types of rarefied gas flows thoroughly studied. Nevertheless, still there are weakly explored domains in the RGD, and the problem of correct slip boundary conditions in reacting flows with coupled vibrational-chemical gas-phase kinetics and heterogeneous reactions is one of such examples.

In continuum approaches, correct description of gas-surface interaction requires incorporating velocity slip and temperature jump as boundary conditions. These conditions, representing the "slip effect", become significant as gas rarefaction increases, allowing to extend the limits of applicability of continuum approaches for nonequilibrium gas mixtures. Various techniques exist to obtain slip boundary conditions for capturing gas-surface interactions. They include modeling slip coefficients from gas-surface simulations, theoretical derivations, or extracting slip conditions from simulations or experiments near the wall [1–9]. Several theoretical methods for derivation of boundary conditions, including a novel state-specific approach based on kinetic boundary condition, have been discussed in details in our previous studies [10–12]. However, incorporating heterogeneous processes in nonequilibrium fluid dynamics, particularly in the detailed state-to-state approach taking into account full vibrational-chemical coupling [13], remains challenging. Attempts have been made to include these processes in theoretical techniques based on both one-temperature and multi-temperature approaches [14–17] but faced limitations in accurate implementing and extending them to state-specific models. A new approach that addresses these limitations has been developed in [12], and the present work is aimed at further extending and assessing the slip conditions derived in [12].

The objectives of this study are: 1) to present briefly the novel approach developed recently by the authors to derive slip boundary conditions for state-to-state flow simulations, and to improve it by ensuring the constraint of zero normal mass flux; 2) to discuss the differences between the original and improved slip conditions and estimate their effect in a nonequilibrium air flow along stagnation line; 3) to evaluate the effect of diffusion model on the flow parameters and heat transfer; 4) to study the influence of momentum accommodation coefficients on the temperature, mixture composition and heat fluxes.

2 State-specific slip boundary conditions

In this section, we briefly discuss the approach recently developed by the authors for deriving slip boundary conditions with respect to heterogeneous reactions [12] and provide its further extension. Here and further, the mixture is described within the framework of the detailed state-to-state (STS) approximation [13] treating all molecular vibrational states as separate chemical species and taking into account all types of vibrational energy transitions coupled to chemical reactions as relaxation

mechanisms. Such an approach is capable to capture strong nonequilibrium effects and deviations of vibrational distributions from quasistationary. However, all the assumptions can be also applied to both one- and multi-temperature approaches, which are less detailed but more computationally efficient.

2.1 KINETIC BOUNDARY CONDITION MODELING

The main feature of the developed approach for evaluating gas-dynamic variables on the wall [10, 12] is the transition from a microscopic to a macroscopic description. This method is similar to the derivation of transport equations from the Boltzmann equation, and further details can be found in [10–12]. Therefore, the microscopic boundary condition, or the kinetic boundary condition, is essential for further derivation. In the STS framework accounting for complex chemical interactions with a solid wall, its form is as follows [12]:

$$(1)\quad f^{+}_{cij}(\mathbf{r},\mathbf{u}_c,t)u_{cn}|_{u_{cn}>0} = -\sum_{l}\int\limits_{u'_{cn}<0} f^{-}_{cil}(\mathbf{r},\mathbf{u}'_c,t)u'_{cn}T^{cij}_{l}(\mathbf{u}_c,\mathbf{u}'_c)\mathrm{d}\mathbf{u}'_c - \sum_{dkl,dk\neq ci}\gamma^{ci}_{dk}\int\limits_{u'_{dn}<0} f^{-}_{dkl}(\mathbf{r},\mathbf{u}'_d,t)u'_{dn}\tilde{T}^{cij}_{dkl}(\mathbf{u}_c,\mathbf{u}'_d)\mathrm{d}\mathbf{u}'_d,$$

where $f^{+}_{cij}(\mathbf{r},\mathbf{u}_c,t)$, $f^{-}_{cij}(\mathbf{r},\mathbf{u}'_c,t)$ are distribution functions of reflected and incident particles of chemical species c at the vibrational level i and rotational level j; $\mathbf{u}_c$ and $\mathbf{u}'_c$ are the molecular velocities of reflected and incident particles; u_{cn} is the velocity component normal to the surface; γ^{ci}_{dk} is the probability, independent of the rotational state, that particle of chemical species d with vibrational level k changes its chemical species and vibrational state to ci; $T^{cij}_{l}(\mathbf{u}_c,\mathbf{u}'_c)$ and $\tilde{T}^{cij}_{dkl}(\mathbf{u}_c,\mathbf{u}'_d)$ are the scattering kernels. The kernels, as the probability densities, must satisfy normalization conditions, which are the following [12]:

$$(2)\qquad \sum_{j}\int\limits_{u_{cn}>0} T^{cij}_{l}(\mathbf{u}_c,\mathbf{u}'_c)\mathrm{d}\mathbf{u}_c = 1 - \sum_{dk,dk\neq ci}\gamma^{dk}_{ci},$$

$$(3)\qquad \sum_{j}\int\limits_{u_{cn}>0} \tilde{T}^{cij}_{dkl}(\mathbf{u}_c,\mathbf{u}'_d)\mathrm{d}\mathbf{u}_c = 1.$$

The second normalization condition is obtained based on the assumption that the scattering kernel $\tilde{T}^{cij}_{dkl}$ is diffusive.

The main difference of the approach proposed in [12] from its original form [10, 11] can be observed in the additional terms in the RHS of Eqs. (1), (2). These terms

are connected to the gain (1) and loss (2) of particles due to wall chemical reactions and vibration excitation/deactivation. The latter processes are included via probabilities γ_{dk}^{ci}. Such an approach provides a correct description of surface non-equilibrium processes, in contrast to the approach presented in [10, 11] and other similar theoretical works [14, 16–18]. For more details, please refer to [12].

In this approach, neglecting the normal velocity component near the wall results in the following balance law:

$$\sum_{ci} n_{ci}\mathbf{V}_{ci}\cdot\mathbf{n}=0. \tag{4}$$

Note that such a relation is not valid if desorption and adsorption processes are accounted for [12]. Here, n_{ci} is the number density of chemical species c in the vibrational state i, $\mathbf{V}_{ci}$ is the diffusion velocity of the same species ci. The relation can be understood as the conservation of the total number flux near the solid wall at given position and time moment. However, in most cases, only the conservation of mass flux is required, which can be achieved numerically within this approach but cannot be derived theoretically.

Therefore, it is useful to develop an approach that ensures mass flux conservation. Such an approach can be based on the following kinetic boundary condition:

$$\begin{aligned} m_c f_{cij}^{+}(\mathbf{r},\mathbf{u}_c,t)u_{cn}|_{u_{cn}>0} = -m_c\sum_{l}\int\limits_{u'_{cn}<0} f_{cil}^{-}(\mathbf{r},\mathbf{u}'_c,t)u'_{cn}T_l^{cij}(\mathbf{u}_c,\mathbf{u}'_c)\mathrm{d}\mathbf{u}'_c \\ -\sum_{dkl,dk\neq ci} m_d\,\gamma_{dk}^{ci}\int\limits_{u'_{dn}<0} f_{dkl}^{-}(\mathbf{r},\mathbf{u}'_d,t)u'_{dn}\tilde{T}_{dkl}^{cij}(\mathbf{u}_c,\mathbf{u}'_d)\mathrm{d}\mathbf{u}'_d, \end{aligned} \tag{5}$$

where m_c is the mass of particle c. The normalization conditions for the kernels are the same. After integrating over the half-space, the condition can be expressed as a relation in the elementary area near the solid wall, regarding the mass flux of reflected particles. This mass flux includes both the mass flux of scattered particles and the mass flux of particles that are transformed into the ci particles. The balance law in such an approach is the conservation of the mass flux near the wall:

$$\sum_{ci}\rho_{ci}\mathbf{V}_{ci}\cdot\mathbf{n}=0, \tag{6}$$

where ρ_{ci} is the density of a given species, $\rho_{ci}=m_c n_{ci}$.

In the subsequent section, the slip conditions will be presented using the two discussed models of kinetic boundary conditions.

2.2 SLIP CONDITIONS FOR DIFFERENT APPROACHES

To derive the slip expressions for the Navier-Stokes approximation, it is necessary to specify the scattering kernel and the first-order distribution function [13, 19]. Here, we consider only the Maxwell scattering kernel $T_{l,M}^{cij}$, whereas the expressions based on the Cercignani-Lampis kernel can be found in [12]. The form of the kernel in the case of the STS approximation, while accounting for possible particle loss, is as follows:

$$T_{l,M}^{cij}(\mathbf{u}_c, \mathbf{u}_c') = (1-\sigma_{ci})\delta_{lj}\delta(\mathbf{u}_c' - \mathbf{u}_c + 2u_{cn}\mathbf{n}) + \Big(\sigma_{ci} - \sum_{dk, dk\neq ci}\gamma_{ci}^{dk}\Big)\frac{2}{\pi}\Big(\frac{m_c}{2kT^w}\Big)^2 \frac{s_j^{ci}u_{cn}}{Z_{rot,ci}(T^w)}\exp\Big(-\frac{m_c u_c^2}{2kT^w} - \frac{\varepsilon_j^{ci}}{kT^w}\Big). \tag{7}$$

Here, T^w is the wall temperature; σ_{ci} is the tangential accommodation coefficient which represents the fraction of particles of ci species that are diffusely reflected (later, the species dependence will be omitted); k is the Boltzmann constant; s_j^{ci} is the rotational statistical weight; $Z_{rot,ci}$ is the rotational partition function depending on the vibrational state i; ε_j^{ci} is the particle rotational energy.

The slip boundary conditions can be expressed in terms of state-specific transport coefficients, including multi-component diffusion and thermal diffusion coefficients D_{cidk} and $D_{T,ci}$, the thermal conductivity coefficient λ' (which includes only contributions of translational and rotational modes, λ_{tr}' and λ_{rot}), the shear and bulk viscosity coefficients μ and ζ, and the relaxation pressure p_{rel} [10]. Corresponding effective transport coefficients introduced additionally for each chemical species and vibrational state, namely $\lambda_{ci}' = \lambda_{tr,ci}' + \lambda_{rot,ci}$, μ_{ci}, ζ_{ci}, and $p_{rel,ci}$, are also used in the expressions for the sake of convenience. Further information on definitions and derivation of effective and true transport coefficients can be found in [10,13]. Besides that, it is convenient to write the expressions in terms of diffusion velocity $\mathbf{V}_{ci}$, mass flux $\mathbf{J}_{ci}$ and viscous stress tensor $\mathbf{P}$:

$$\mathbf{V}_{ci} = -\sum_{dk} D_{cidk}\mathbf{d}_{dk} - D_{T,ci}\nabla \ln T, \qquad \mathbf{J}_{ci} = \rho_{ci}\mathbf{V}_{ci}, \tag{8}$$

$$\mathbf{P} = (p - \zeta\nabla\cdot\mathbf{v} - p_{rel})\mathbf{I} - 2\mu\mathbf{S}, \tag{9}$$

where T is the gas temperature; p is the pressure, $\mathbf{S}$ is the traceless symmetric part of the strain rate tensor; $\mathbf{I}$ is the unit tensor; $\mathbf{d}_{ci}$ is the diffusive driving force for each chemical species c and vibrational state i.

The procedure described in [10, 12] yields the following relations for the wall mass fluxes, which correspond to the approaches based on Eqs. (1) and (5):

$$\left(2-\sum_{dk,dk\neq ci}\gamma_{ci}^{dk}\right)\mathbf{J}_{ci}\cdot\mathbf{n}=-\frac{\sum_{dk,dk\neq ci}\gamma_{ci}^{dk}\rho_{ci}}{n\sqrt{2\pi m_c kT}}\left(p+P_{nn,ci}\right)$$
$$-\sum_{dk,dk\neq ci}\gamma_{dk}^{ci}\frac{m_c}{m_d}\mathbf{J}_{dk}\cdot\mathbf{n}+\frac{1}{\sqrt{2\pi kT}}\sum_{dk,dk\neq ci}\gamma_{dk}^{ci}\frac{m_c\rho_{dk}}{n\sqrt{m_d^3}}\left(p+P_{nn,dk}\right); \tag{10}$$

$$\left(2-\sum_{dk,dk\neq ci}\gamma_{ci}^{dk}\right)\mathbf{J}_{ci}\cdot\mathbf{n}=-\frac{\sum_{dk,dk\neq ci}\gamma_{ci}^{dk}\rho_{ci}}{n\sqrt{2\pi m_c kT}}\left(p+P_{nn,ci}\right)$$
$$-\sum_{dk,dk\neq ci}\gamma_{dk}^{ci}\mathbf{J}_{dk}\cdot\mathbf{n}+\frac{1}{\sqrt{2\pi kT}}\sum_{dk,dk\neq ci}\gamma_{dk}^{ci}\frac{\rho_{dk}}{n\sqrt{m_d}}\left(p+P_{nn,dk}\right), \tag{11}$$

where $c=1,\ldots,L,\ i=0,\ldots,L_c$, and L_c is the number of vibrational states of c particle, L is the number of components in the mixture; n is the total number density; $P_{nn,ci}$ is defined as $P_{nn,ci}=p-\ 2\mu_{ci}S_{nn}-\zeta_{ci}\nabla\ \cdot\ \mathbf{v}-p_{rel,ci}$. A distinction can be observed in the relations, specifically in the presence of the ratio m_c/m_d in the last two terms of the RHS.

The velocity slip is the same for both considered approaches:

$$v_l=\frac{\sqrt{\frac{\pi}{2kT}}\frac{2-\sigma}{\sigma}\,2\mu\,S_{ln}+\sum_{ci}n_{ci}\sqrt{m_c}\left(\frac{\lambda'_{tr,ci}}{5kn}\frac{\partial\ln T}{\partial\tau_l}-\mathbf{V}_{ci}\cdot\boldsymbol{\tau}_l\right)}{\sum_{ci}\frac{n_{ci}}{2nkT}\sqrt{m_c}\left(p+P_{nn,ci}\right)},\ l=1,2. \tag{12}$$

Temperature jumps, on the other hand, vary, and their simplified expressions based on the balance laws (4) and (6) are the following:

$$\frac{T}{T^w}=\frac{\sigma\sqrt{\frac{2}{\pi kT}}\sum_{ci}\frac{n_{ci}}{2n\sqrt{m_c}}\left(1+\frac{m_c v^2}{4kT^w}\right)\cdot\left(p+P_{ci,nn}\right)}{-\frac{(2-\sigma)\lambda'}{2k}\frac{\partial\ln T}{\partial n}+\sigma\sqrt{\frac{2}{\pi kT}}\,Y}, \tag{13a}$$

$$Y=\sum_{ci}\frac{3n_{ci}}{2n}\left(\frac{-\frac{p}{3}+\mu_{ci}S_{nn}+P_{ci,nn}}{\sqrt{m_c}}+\frac{\sqrt{m_c}c_{rot,ci}T(\mathrm{f}_{ci,01}\nabla\cdot\mathbf{v}+\mathrm{g}_{ci,01})}{3}\right); \tag{13b}$$

$$\frac{T}{T^w}=\frac{\sigma\sqrt{\frac{2}{\pi kT}}\sum_{ci}\frac{\rho_{ci}}{2n\sqrt{m_c}}\left(1+\frac{m_c v^2}{4kT^w}\right)\cdot\left(p+P_{ci,nn}\right)}{-(2-\sigma)\sum_{ci}\frac{\rho_{ci}}{n}\frac{\lambda'_{ci}}{2k}\frac{\partial\ln T}{\partial n}+\sigma\sqrt{\frac{2}{\pi kT}}\,Z}, \tag{14a}$$

$$Z=\sum_{ci}\frac{3\rho_{ci}}{2n}\left(\frac{-\frac{p}{3}+\mu_{ci}S_{nn}+P_{ci,nn}}{\sqrt{m_c}}+\frac{\sqrt{m_c}c_{rot,ci}T(\mathrm{f}_{ci,01}\nabla\cdot\mathbf{v}+\mathrm{g}_{ci,01})}{3}\right). \tag{14b}$$

In the above relations, $c_{rot,ci}$ is the rotational specific heat depending on the vibrational state; $\mathrm{f}_{ci,01}$ and $\mathrm{g}_{ci,01}$ are the expansion coefficients which appear in the expressions for transport coefficients. The algorithm for the evaluation of coefficients $\mathrm{f}_{ci,01}$ and $\mathrm{g}_{ci,01}$ (as well as for all transport coefficients) according to the first-order Chapman–Enskog approximation includes expansion of the first-order distribution function into the series of orthogonal Sonine and Waldmann–Trübenbacher polynomials and reducing integral equations to the linear algebraic transport systems [13].

The model based on slip conditions (10) and (13) will be hereafter referred to as Model I, while the other model based on Eqs. (11) and (14) will be referred to as Model II.

2.3 Diffusion velocity models

As one can observe, the slip conditions for species mass fluxes (10) and (11) depend on the diffusion velocity. The rigorous state-specific relation (8) requires the knowledge of numerous parameters. Moreover, in such a case, the boundary conditions will form a system of non-linear equations that must be solved at each iteration. That is why it is preferable to employ simplified models for the diffusion velocity. One of the commonly used models is the traditional Fick law:

$$\rho_{ci}\mathbf{V}_{ci} = -\rho D_{ci}\nabla\cdot\left(\frac{\rho_{ci}}{\rho}\right), \qquad D_{ci} = \frac{1-n_{ci}/n}{\sum\limits_{dk} n_{dk}/(n\mathcal{D}_{cidk})}, \tag{15}$$

where D_{ci} is the effective diffusion coefficient, $\mathcal{D}_{cidk}$ are binary diffusion coefficients.

The Hirschfelder-Curtiss (HC) [20] approximation is another simplified model for the diffusion velocity, which can be used as an alternative to (15):

$$n_{ci}\mathbf{V}_{ci} = -nD^{*}_{ci}\mathbf{d}_{ci}, \qquad D^{*}_{ci} = \frac{1-\rho_{ci}/\rho}{\sum\limits_{dk,dk\neq ci} n_{dk}/(n\mathcal{D}_{cidk})}. \tag{16}$$

The Fick law is commonly used in fluid dynamics but originally it was limited to binary mixtures [21, 22]; expression (15) represents its generalization. However, it still neglects thermal and barodiffusion as well as cross-coupling between gradients of various species mass fractions. The Hirschfelder–Curtiss law partially overcomes these limitations since it includes species molar fractions and diffusive driving forces, similarly to initial definition (8). Thus, the HC law is treated here as more accurate. However, neither of these relations can provide the global mass conservation $\sum_{ci}\rho_{ci}\mathbf{V}_{ci} = 0$. This constraint can be satisfied by adding a correction to the diffusion velocity expressions [21]. Nevertheless, in the present study we do not take into account this modification.

Both Fick and HC diffusion models are assessed in the next section, where we discuss the results of non-equilibrium air flows simulations in the boundary layer in the vicinity of the stagnation point.

3 Air flow in the boundary layer

In this Section we implement the proposed models for slip boundary conditions to numerical simulations of a one-dimensional flow of reacting air mixture along the stagnation line. The effect of various models on the fluid-dynamic variables and heat flux is analysed.

3.1 Governing equations

The one-dimensional flow of a five component N_2/N/O_2/O/NO air mixture in the vicinity of stagnation point is described by the set of governing equations written in the Lees–Dorodnitsyn coordinates [23]:

$$\xi = \int_0^x \rho_e \mu_e v_e dx, \qquad \eta = \frac{v_e}{\sqrt{2\xi}} \int_0^y \rho dy, \tag{17}$$

ξ and η are the coordinates parallel and normal to the body surface; the subscript 'e' refers to the external edge of the boundary layer.

After the transformation of coordinates, the velocity dependence on ξ vanishes, and the set of equations takes the form

$$\begin{aligned} &\frac{\partial^2 y_i}{\partial \eta^2} + \psi \,\mathrm{Sc}\, \frac{\partial y_i}{\partial \eta} = S_i, \qquad i = 1, ..., NumSp, \\ &\frac{\partial^2 T/T_e}{\partial \eta^2} + \psi \,\mathrm{Pr}\, \frac{\partial T/T_e}{\partial \eta} = S_T. \end{aligned} \tag{18}$$

Here, $y_i = \rho_{ci}/\rho$ is the species i mass fraction in frame of the STS approach; they include all vibrational states of molecular species and atomic species; for the present mixture $NumSp = 155$; T/T_e is the temperature normalized to its value T_e at the external boundary layer edge; ψ is the stream function; Sc and Pr are the Schmidt and Prandtl numbers, respectively.

The gas-phase reactions taken into account in the production terms S_i, S_T include vibrational-vibrational (VV) energy transitions, vibrational-translational exchanges in collisions with an atom or a molecule (VT_a, VT_m), state-specific dissociation-recombination and Zeldovich exchange reactions. Rate coefficients of the majority of these reactions depending on the vibrational states are taken from quasi-classical trajectory calculations [24–27]. The details of the gas-phase kinetic scheme are given in Refs. [25, 27].

The heterogeneous reactions at the surface are state-specific recombination reactions according to the Eley-Rideal impact mechanism, proceeding in a collision of a gas-phase atom with an atom adsorbed earlier by the surface (adatom). We take into account recombination of oxygen, nitrogen, and two mechanisms of NO recombination with different pairs atom–adatom. Recombination probabilities are calculated at each iteration based on the approach proposed in [28, 29]. Details of their calculation can be found in [27, 30]. This rigorous procedure is necessary, given that the probabilities depend on both the surface properties and the impinging flux.

3.2 Test cases

Let us specify first the flow parameters at the external edge of the boundary layer (Table 1). These parameters correspond to the conditions behind the bow shock wave

Table 1: External edge flow parameters and surface temperature

Notation	T_e, K	T^w, K	p_e, Pa	β, 1/s
EP1 (85 km)	7000	1000	1000	5000
EP2 (60 km)	9500	1150	17600	3086

near a re-entering space vehicle. The altitude for the considered cases is approximately 85 km and 60 km, with a Mach number of 15. The temperature (T_e), pressure (p_e), and the parameter β (the inverse of the residence time of a gas element in the boundary layer) vary among the sets EP1 and EP2. At the outer edge, the air mixture consists of N_2+N (78.58%), O_2+O (21.38%), and NO (0.04%). The wall temperature on the silica surface, denoted as T^w, is set to 1000 K and 1150 K. Numerical modeling is performed for different test cases of slip boundary conditions; the details of the numerical method are given in Ref. [23]. The models and parameters that are varied in this study include: 1) two different sets of slip conditions: Model I (Eqs. (10) and (13)) and Model II (Eqs. (11) and (14)); 2) two diffusion velocity models: the Fick law (15) and the HC approximation (16); 3) the accommodation coefficient σ takes values from the set $\{0, 0.1, 0.25, 0.5, 0.75, 1\}$.

3.3 Results and discussion

Temperature profiles across the boundary layer are presented in Fig. 1 ($\eta = 0$ corresponds to the wall), and, as can be seen, are barely affected by the chosen type of slip conditions and diffusion velocity model. The most significant difference is observed with the HC model, resulting in an approximate 2% increase in the wall temperature value. The influence of the accommodation coefficient, on the other hand, is rather high. One can observe that as the accommodation coefficient decreases, the

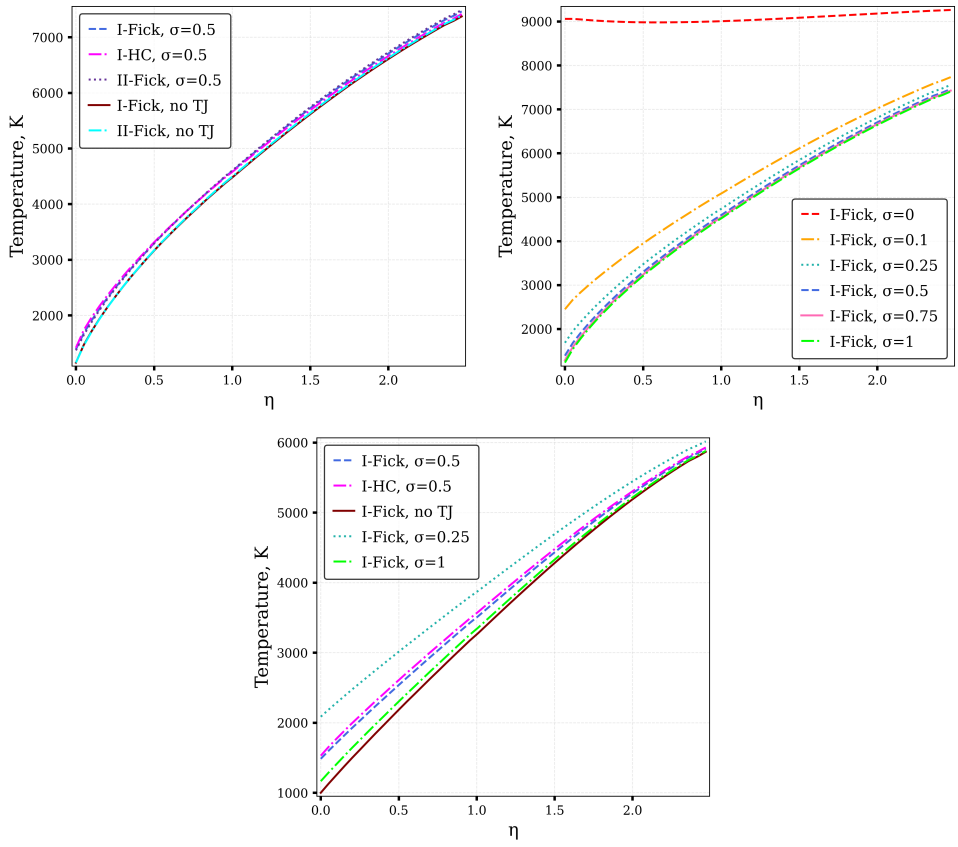

Fig. 1: Temperature profiles. Top – EP2 (60km) case, bottom – EP1 (85km) case.

temperature jump increases; this effect is stronger for $\sigma < 0.5$. This situation corresponds to the conditions when specular scattering dominates over diffuse scattering; $\sigma = 0$ corresponds to purely specular scattering by a solid wall. The latter case corresponds to a thermally insulated wall with no energy exchange, therefore, the temperature remains constant across the boundary layer. The effect of temperature jump is stronger near the wall in the more rarefied case (EP1), as expected. It is worth noting that the temperature jump, as well as the temperature profile in the boundary layer, is affected by the accommodation coefficient more than by the surface catalycity: repeating simulations in the same conditions as in the top-right panel of Fig. 1 but without the gas-surface reactions yields almost the same results, especially for increasing σ values.

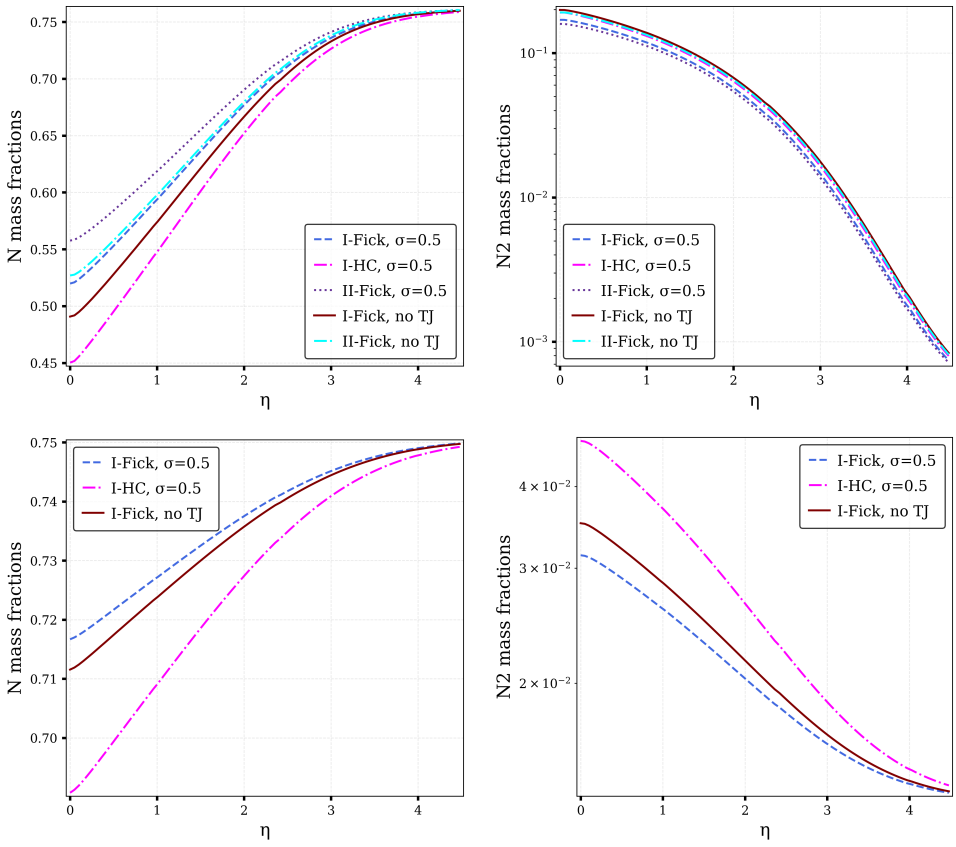

Fig. 2: N and N_2 mass fractions. Top – EP2 (60km) case, bottom – EP1 (85km) case.

Mass fraction variation in the boundary layer is plotted in Figs. 2, 3 and 4 for N, N_2; O, O_2; and NO, respectively. The effect of slip conditions based on two kinetic boundary conditions (1) and (5), and the impact of diffusion model are evaluated for nitrogen atoms and molecules, while the influence of the accommodation coefficients and gas rarefaction is assessed for oxygen, as these effects are primarily observed for the chosen types of mixture species. First of all, we can conclude that using original and modified kinetic boundary conditions yields similar results; maximum variation of up to 7% is observed in N mass fraction at the wall when the temperature jump is taken into account; for other fluid-dynamic variables, the effect is weaker. Therefore, although the results obtained on the basis of improved kinetic boundary condition (5) should be considered as more rigorous, the initial approach developed in [12] still provides good accuracy.

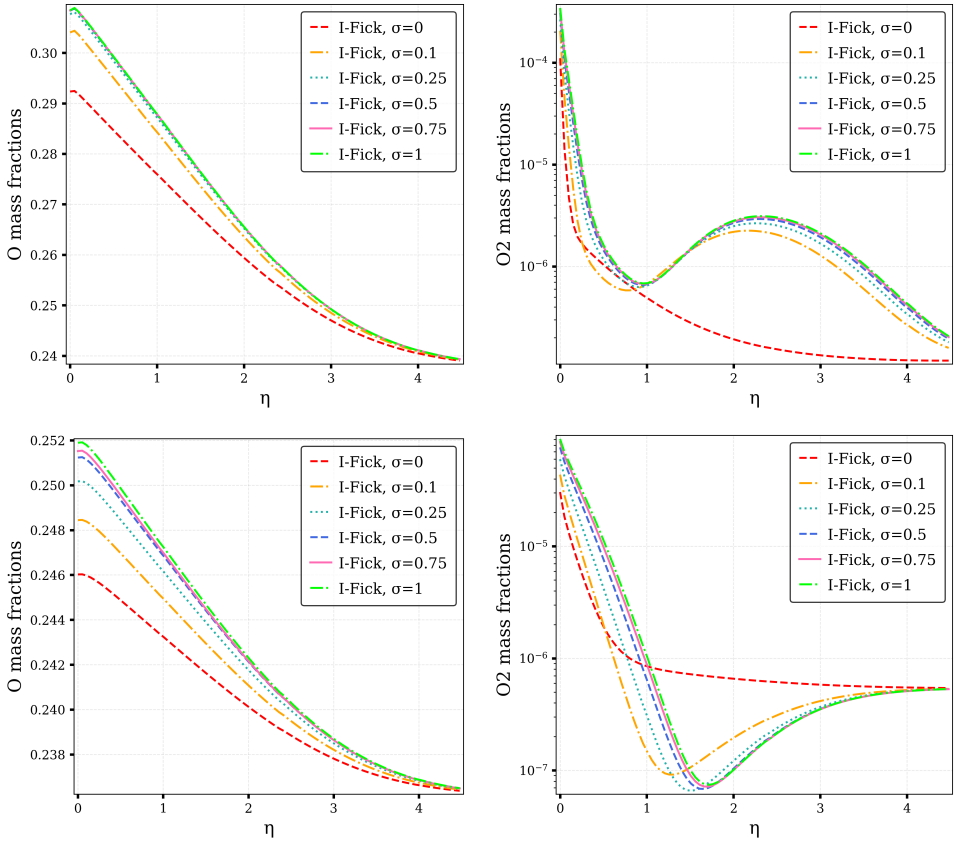

Fig. 3: O and O_2 mass fractions. Top – EP2 (60km) case, bottom – EP1 (85km) case.

The impact of diffusion model is much more significant; for N_2 the discrepancy is up to 50% in the a more rarefied gas (EP1). The diffusion effect is even more important than that of the temperature jump. Based on this analysis, we believe that using the Fick law may lead to noticeable inaccuracy in the mixture composition evaluation. Implementation of the kinetic-theory diffusion model (Eq. (8)) or the relation with correction [21] requires further work and should be studied more thoroughly.

The effect of accommodation coefficient on the mass fraction profiles near the wall is not as significant as observed for the temperature; the biggest difference is found for O_2 molecules (see Fig. 3). The mass fractions show a monotonic behaviour for all species, except for oxygen and NO molecules. In the case of oxygen, the fractions on the wall decrease with a decrease in the accommodation coefficient.

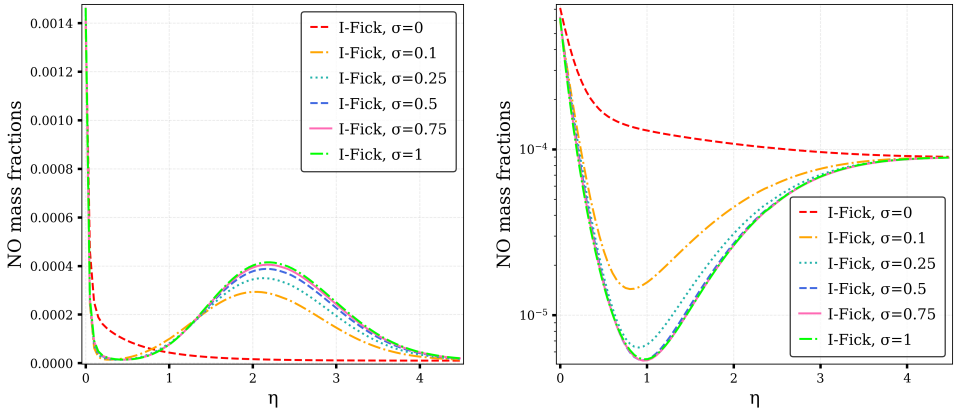

Fig. 4: NO mass fractions. Left – EP2 (60km) case, right – EP1 (85km) case.

An interesting effect obtained for $\sigma = 0$ (purely specular scattering) may be observed for oxygen molecules. In this case, the distributions exhibit a consistent decrease in the shown boundary layer region. A similar effect is also observed for NO distributions (see Fig. 4). This behaviour is connected to the fact that the temperature is constant across the boundary layer, so the main influence is provided by the heterogeneous recombination, resulting in the observed profiles. Here as well, the temperature jump model provides stronger effects with increasing gas rarefaction.

Let us evaluate the influence of the considered models on the total heat flux in the boundary layer (Fig. 5). The two types (I and II) of slip conditions have relatively minor effects, while the influence of the diffusion model is more significant. The difference is approximately 6% when considering or neglecting the temperature jump. The effect of different σ values on the total fluxes is opposite to their influence on temperature profiles: the total flux increases with an increase in σ values. As expected, when $\sigma = 0$, the total heat flux becomes zero since the wall is thermally insulated and the temperature is constant across the layer.

4 Conclusions

An improved version of the kinetic boundary condition is proposed that ensures conservation of the mass flux near the surface in the case of heterogeneous recombination reactions and vibrational energy transitions. Using this boundary condition and Maxwell scattering kernel wall mass fluxes, velocity slip and temperature jump are derived in the state-to-state approximation allowing for coupling of vibrational-chemical kinetics with fluid dynamics. The models are implemented into

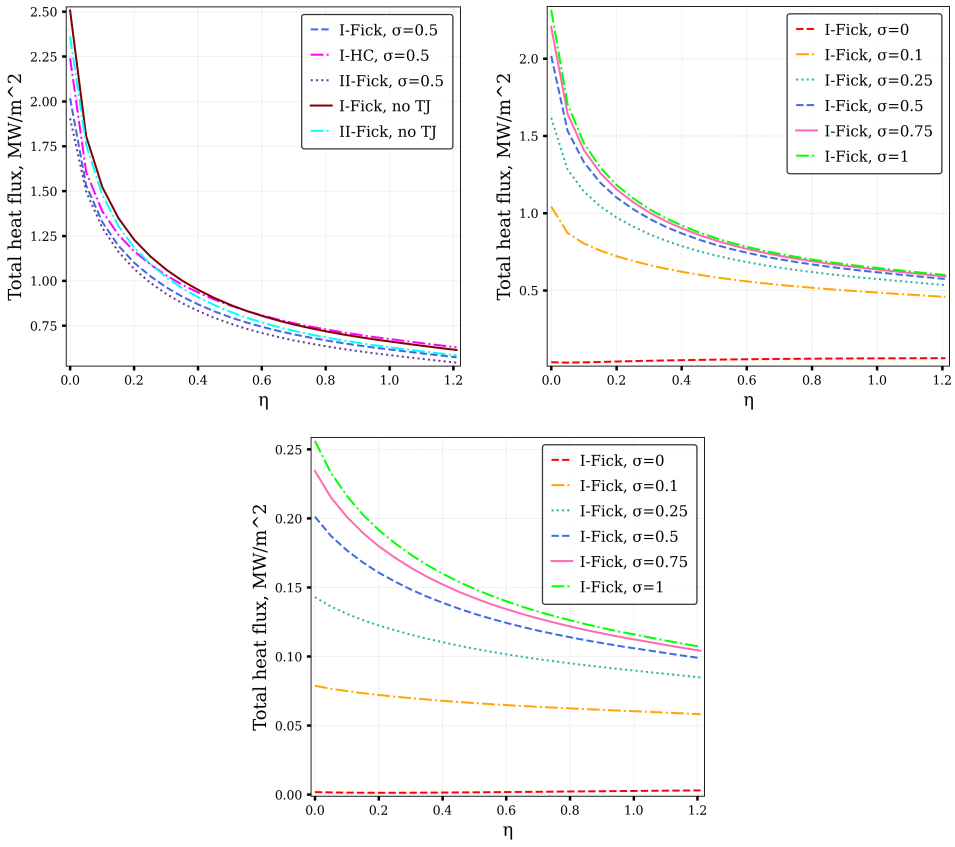

Fig. 5: Total heat flux. Top – EP2 (60km) case, bottom – EP1 (85km) case.

the code simulating air flows in a boundary layer near stagnation point; several test cases corresponding to various altitudes and accommodation coefficients are studied. Two diffusion models are assessed: the approximate Fick law and a more accurate Hirschfelder–Curtiss model. It is shown that using simplified diffusion models may considerably alter mixture composition near the surface. In the future studies we plan to implement more rigorous diffusion models based on the kinetic theory.

The results obtained on the basis of the improved kinetic boundary condition are compared to those calculated in the frame of the previously developed approach. The discrepancy is small, less than the effect of diffusion model. Therefore, the initial kinetic boundary condition still can be used without considerable loss of accuracy. The choice of accommodation coefficients strongly affects gas properties near the wall:

fluid-dynamic variables vary considerably for $\sigma < 0.5$ (when specular scattering dominates), but with further increase in σ they remain almost unchanged. The effect of temperature jump becomes stronger for more rarefied flows. Due to the substantial impact of momentum accommodation coefficient, it is interesting to investigate alternative models of particle interaction with solid walls, such as the Cercignani-Lampis and Lord scattering kernels including also energy accommodation. Furthermore, conducting a comparative analysis with various phenomenological models of gas-surface interaction is crucial.

ACKNOWLEDGEMENTS

This study is supported by the Russian Science Foundation, project 22-11-00078.

REFERENCES

[1] H. GRAD (1949) On the kinetic theory of rarefied gases. *Communications on Pure and Applied Mathematics* **2** 331-407.

[2] G. N. PATTERSON (1956) "Molecular Flow of Gases". Wiley, New York.

[3] S. TAKATA, S. YASUDA, S. KOSUGE, K. AOKI (2003) Numerical analysis of thermal-slip and diffusion-slip flows of a binary mixture of hard-sphere molecular gases. *Physics of Fluids* **15** 3745-3766.

[4] C.E. SIEWERT (2003) Viscous-slip, thermal-slip, and temperature-jump coefficients as defined by the linearized boltzmann equation and the Cercignani–Lampis boundary condition. *Physics of Fluids* **15** 1696-1701.

[5] F. SHARIPOV, D. KALEMPA (2003) Velocity slip and temperature jump coefficients for gaseous mixtures. I. Viscous slip coefficient. *Physics of Fluids* **15** 1800-1806.

[6] A.A. STEPANENKO, V.A. ZAZNOBA, V.M. ZHDANOV (2019) Boundary slip phenomena in multicomponent gas mixtures. *Physics of Fluids* **31** 062105.

[7] N.N. NGUYEN, I. GRAUR, P. PERRIER, S. LORENZANI (2020) Variational derivation of thermal slip coefficients on the basis of the Boltzmann equation for hard-sphere molecules and Cercignani–Lampis boundary conditions: Comparison with experimental results. *Physics of Fluids* **32** 102011.

[8] R. LI, Y, YANG (2023) Slip and jump coefficients for general gas–surface interactions according to the moment method. *Physics of Fluids* **35** 032010.

[9] K. AOKI, V. GIOVANGIGLI (2019) Kinetic model of adsorption on crystal surfaces. *Physical Review E* **99** 052137.

[10] L. SHAKUROVA, E. KUSTOVA (2022) State-specific boundary conditions for nonequilibrium gas flows in slip regime. *Physical Review E* **105** 034126.

[11] L.A. SHAKUROVA, E.V. KUSTOVA (2022) Boundary conditions for fluid-dynamic parameters of a single-component gas flow with vibrational deactivation on a solid wall. *Vestnik St. Petersburg University, Mathematics* **55** 249256.

[12] L. SHAKUROVA, E. KUSTOVA (2023) Slip boundary conditions for gas mixture flows with state-to-state vibrational-chemical kinetics. *AIP Conference Proceedings* [accepted].

[13] E. NAGNIBEDA, E. KUSTOVA (2009) "Nonequilibrium Reacting Gas Flows. Kinetic Theory of Transport and Relaxation Processes". Springer Verlag, Berlin.

[14] CARL SCOTT (1973) Wall boundary equations with slip and catalysis for multicomponent, nonequilibrium gas flows. *NASA TM X-58111*.

[15] B.A. KIRYUTIN, G.A. TIRSKII (1996) Slip boundary conditions on a catalytic surface in a multicomponent gas flow. *Fluid Dynamics* **31** 134143.

[16] B. XU AND Y. JU (2006) Theoretical and numerical studies of non-equilibrium slip effects on a catalytic surface. *Combustion Theory and Modelling* **10** 961-979.

[17] A. ZADE, M. RENKSIZBULUT, J. FRIEDMAN (2008) Slip/jump boundary conditions for rarefied reacting/non-reacting multi-component gaseous flows. *International Journal of Heat and Mass Transfer* **51** 5063-5071.

[18] R. GUPTA, C. SCOTT, J. MOSS (1985) Slip-boundary equations for multicomponent nonequilibrium airflow. *NASA Technical Paper 85820*.

[19] J.H. FERZIGER, H.G. KAPER (1972) "Mathematical Theory of Transport Processes in Gases". North-Holland Publishing Co., Amsterdam, London.

[20] J.O. HIRSCHFELDER, C.F. CURTISS, R.B. BIRD (1964) "Molecular theory of gases and liquids". Wiley, New York.

[21] V. GIOVANGIGLI (1991) Convergent iterative methods for multicomponent diffusion. *IMPACT of Computing in Science and Engineering* **3** 244-276.

[22] E. GIACOMAZZI, F.R. PICCHIA, N. ARCIDIACONO (2008) A review of chemical diffusion: Criticism and limits of simplified methods for diffusion coefficient calculation. *Combustion Theory and Modelling* **12** 135-158.

[23] I. ARMENISE, E. KUSTOVA (2013) State-to-state models for CO_2 molecules: from the theory to an application to hypersonic boundary layers. *Chemical Physics* **415** 269-281.

[24] I. ARMENISE, M. CAPITELLI (2005) State to state vibrational kinetics in the boundary layer of an entering body in earth atmosphere: particle distributions and chemical kinetics. *Plasma Sources Science and Technology* **14** S9.

[25] I. ARMENISE, F. ESPOSITO (2015) N_2, O_2, NO state-to-state vibrational kinetics in hypersonic boundary layers: The problem of rescaling rate coefficients to uniform vibrational ladders. *Chemical Physics* **446** 30-46.

[26] F. ESPOSITO, I. ARMENISE (2017) Reactive, inelastic, and dissociation processes in collisions of atomic oxygen with molecular nitrogen. *The Journal of Physical Chemistry A* **121** 6211-6219.

[27] I. ARMENISE, F. ESPOSITO (2021) N+O_2(v) collisions: reactive, inelastic and dissociation rates for state-to-state vibrational kinetic models. *Chemical Physics* **551** 111325.

[28] F. NASUTI, M. BARBATO, C. BRUNO (1996) Material-dependent recombination modeling for hypersonic flows. *Journal of Thermophysics and Heat Transfer* **10** 131-136.

[29] M. BARBATO, S. REGGIANI, C. BRUNO, J. MUYLAERT (2000) Model for heterogeneous catalysis on metal surfaces with applications to hypersonic flows. *Journal of Thermophysics and Heat Transfer* **14** 412-420.

[30] I. ARMENISE, M. BARBATO, M. CAPITELLI, E.V. KUSTOVA (2006) State-to-state catalytic models, kinetics and transport in hypersonic boundary layers. *Journal of Thermophysics and Heat Transfer* **20** 465-476.